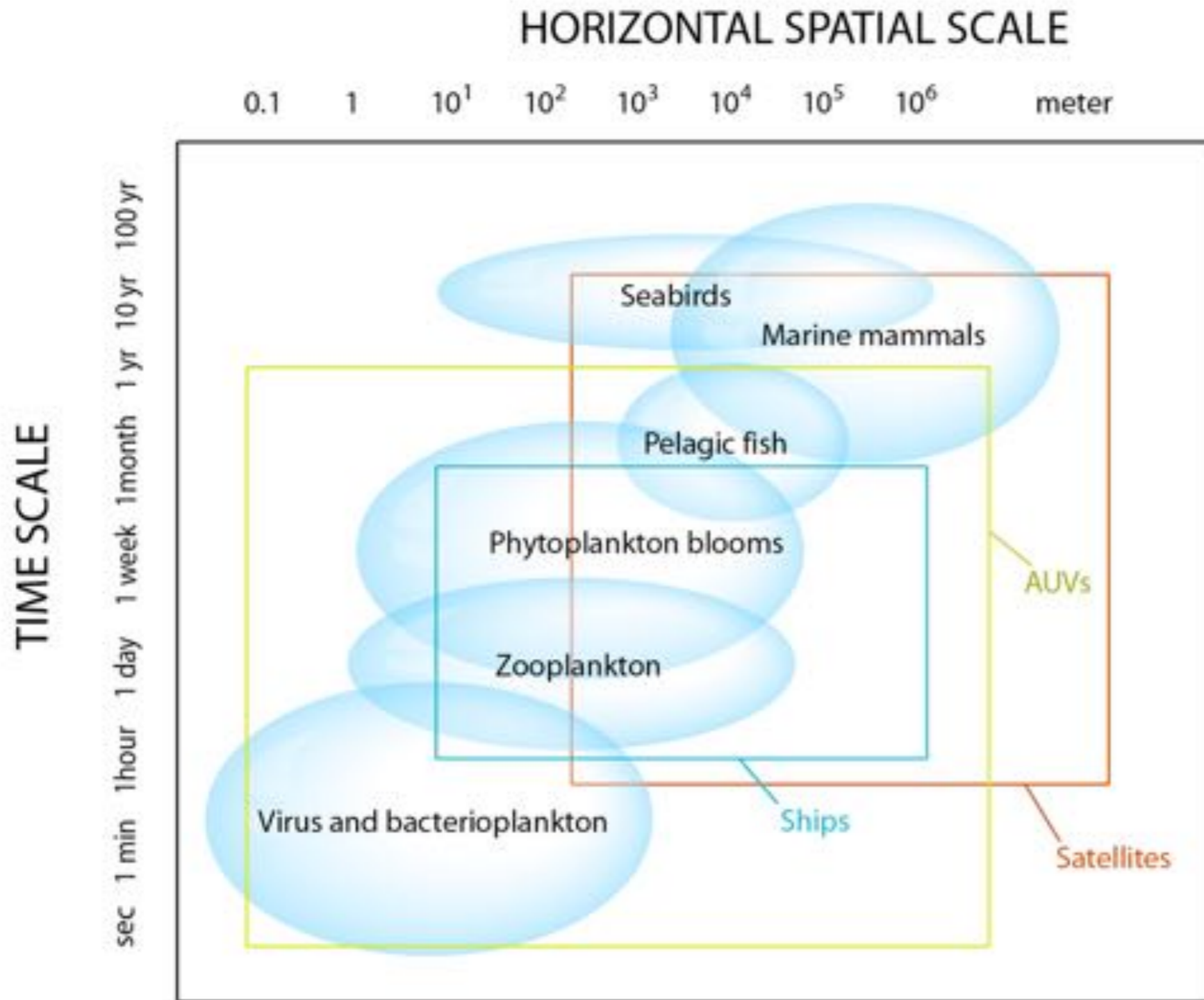


Hyperspectral imaging above & in water - applications

Geir Johnsen, AMOS, Dept biology, NTNU

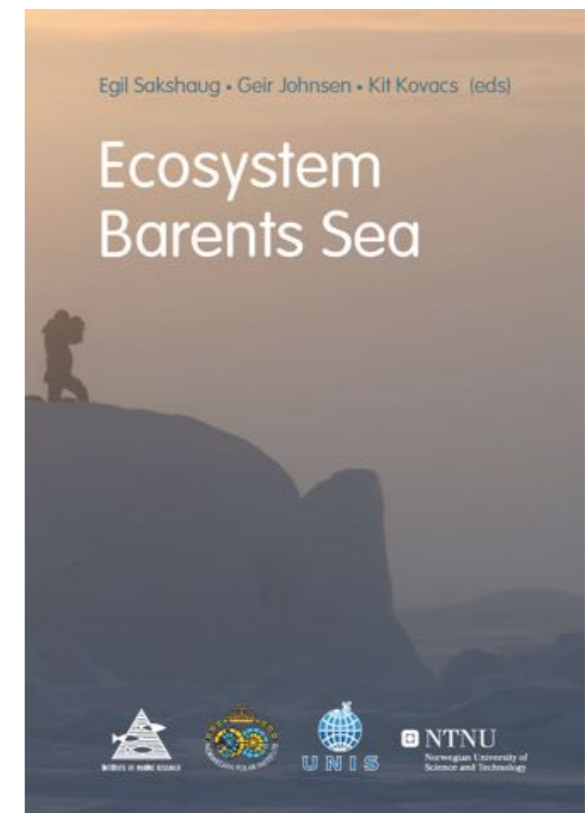
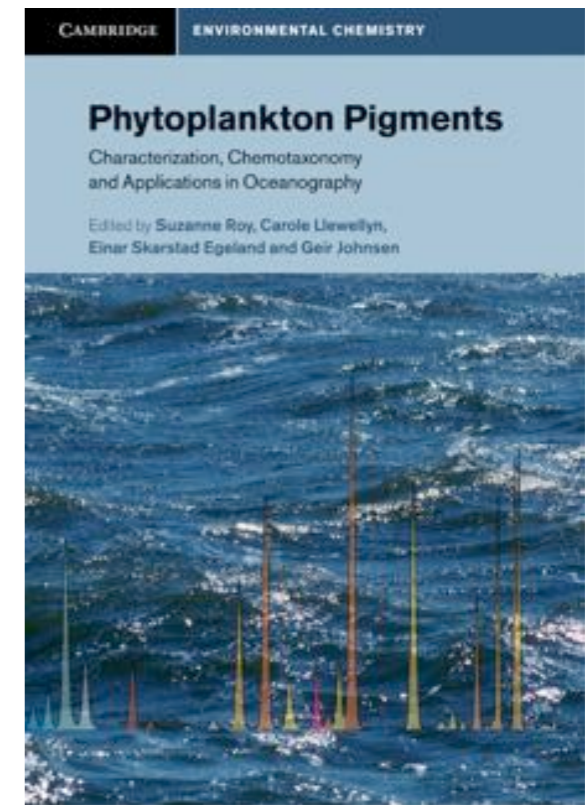


How to sample ocean colour (passive sensors) in time and space



13 major pigment groups of phytoplankton – different hyperspectral optical fingerprints

Raw counts to radiance to reflectance: Not trivial



Challenges using passive sensors

How to identify, map & monitor different PG of phytoplankton

Satellites:

PROS:

1. Cover large areas
2. Time-series
3. Operational (management and decision making, eg. HAB)
4. Creates maps easy understandable for end user

CONS:

1. Restricted to sea surface
2. Dependent on sun and cloud cover
3. Do not discriminate between PGs
4. Dependent on local algorithms reg atm/water properties

Mid Norway: ≈ 70 data lost due to cloud cover

Principles of remote sensing

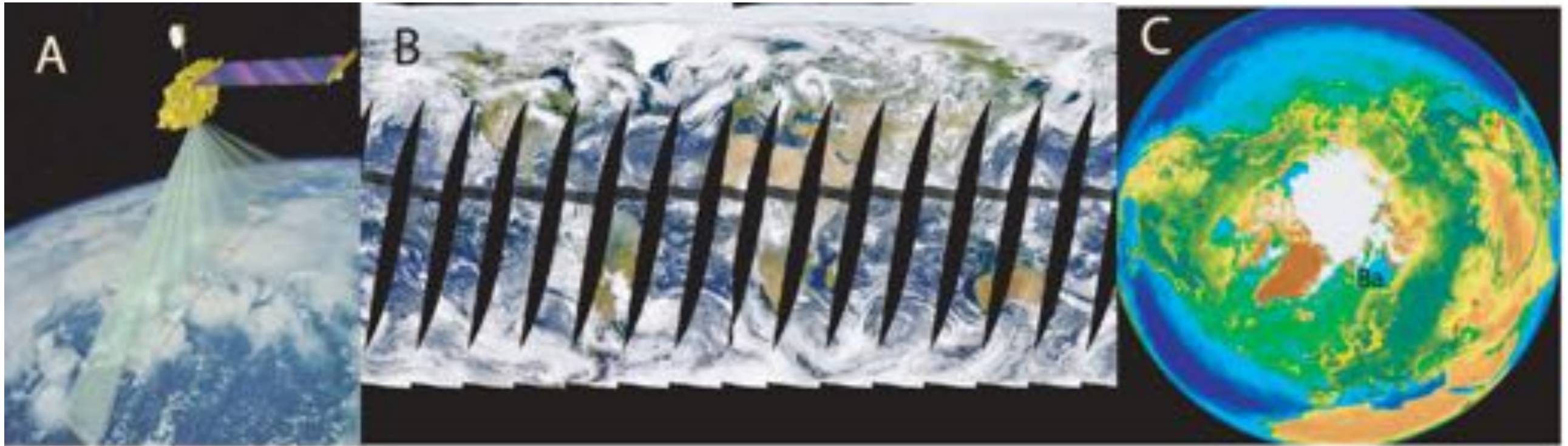
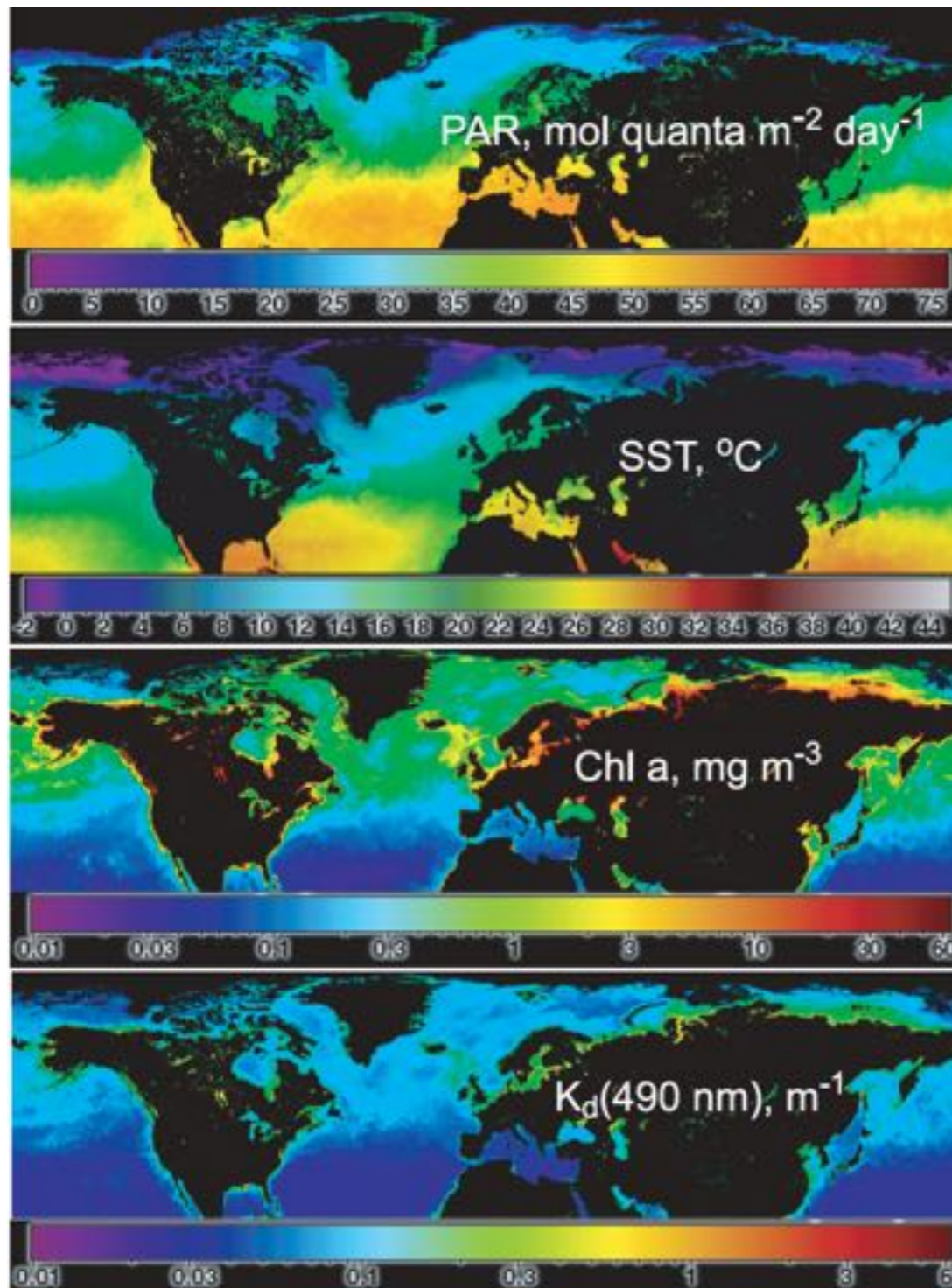


Figure 6.1.

- A. Swath width of the Multi-angle Imaging SpectroRadiometer (MISR) deployed on the Terra satellite. The instrument provides global coverage of the brightness, contrast, and colour of reflected sunlight. The information is used to elucidate the effect of different types of atmospheric particles (aerosols) and clouds on climate. Jet Propulsion Laboratory, NASA.
- B. Fifteen polar orbits (4 August 2007) of the SeaWiFS instrument at 705 km altitude. The swath width is 1502-2806 km. A complete orbit takes approximately 100 minutes, implying global coverage in 25 h (15 orbits x 1.67 h = 25 h).
- C. Northern biosphere image indicating Chla concentration and distribution of sea-ice (annual minimum, only multi-year ice) in August - September. Ba: Barents Sea. B and C: courtesy of G. C. Feldman (SeaWiFS project, NASA).

Remotely sensed E_{PAR} , SST, Chl a and CDOM

(cumulative June-Aug)



E. huxleyi bloom in the Barents Sea - 2004

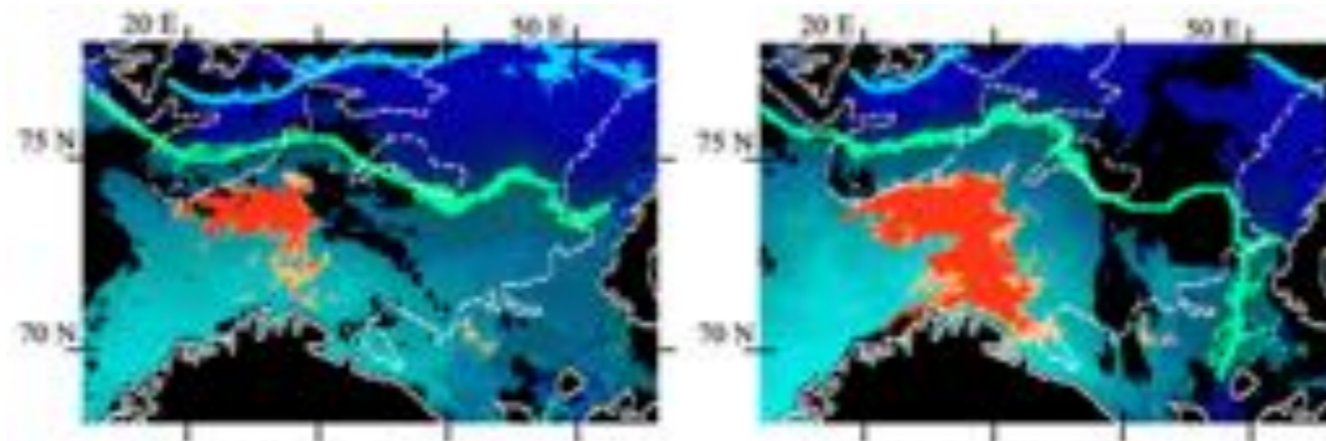


Fig. 9.a Period: 17-Jul to 19-Jul 2004
Area 1: 68,500 km² Area 2: 34,000 km²

Fig. 9.b Period: 26-Jul to 27-Jul 2004
Area 1: 142,000 km² Area 2: 94,500 km²

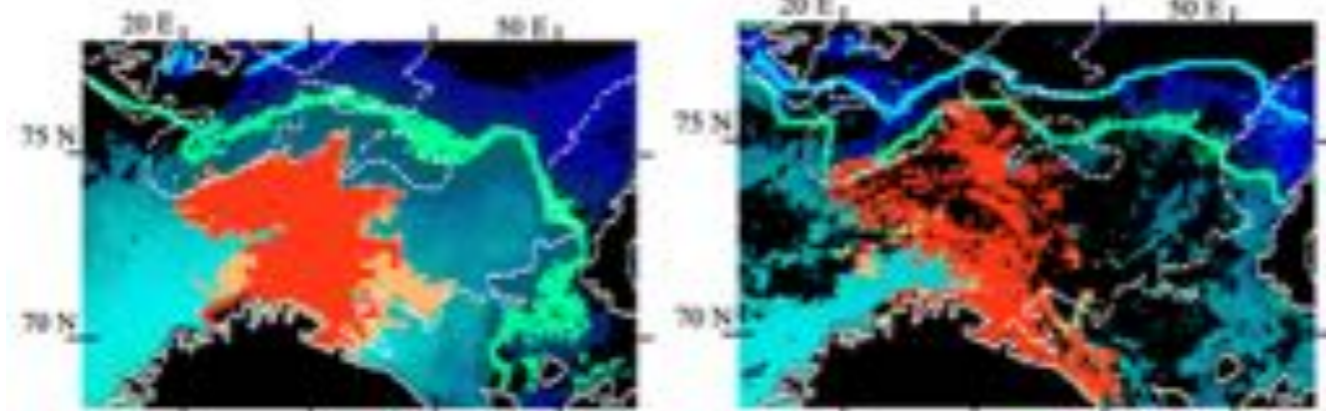


Fig. 9.c Period: 28-Jul to 04-Aug 2004
Area 1: 237,500 km² Area 2: 187,500 km²

Fig. 9.d Period: 13-Aug to 20-Aug 2004
Area 1: 226,000 km² Area 2: 207,000 km²

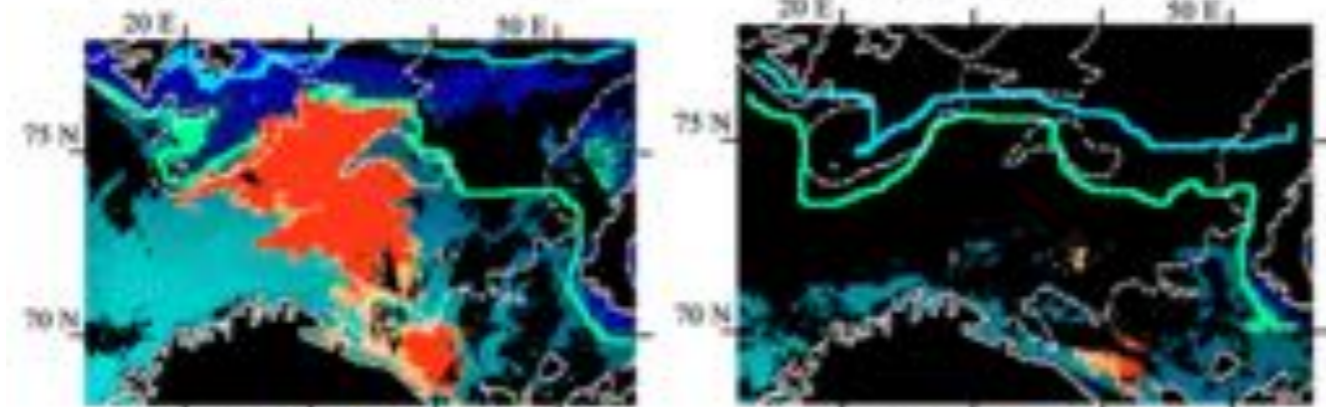
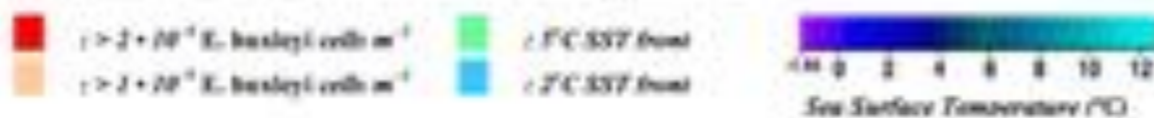


Fig. 9.e Period: 29-Aug to 03-Sep 2004
Area 1: 273,000 km² Area 2: 245,500 km²

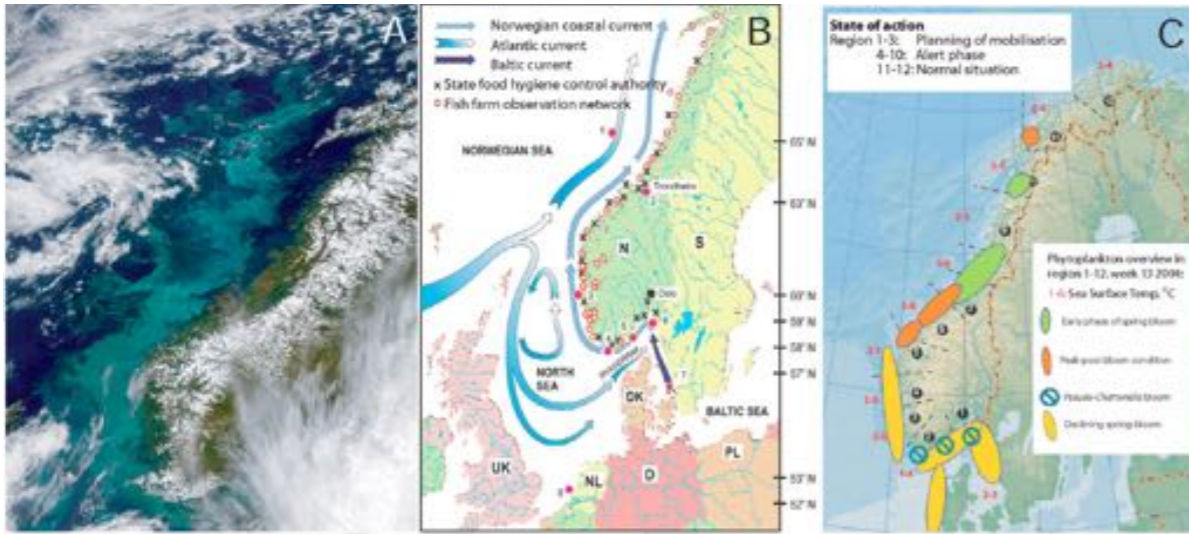
Fig. 9.f Period: 14-Sep to 21-Sep 2004
Area 1: 18,000 km² Area 2: 4,500 km²

Fig. 9.a-f *E. huxleyi* bloom pixels in the year 2004 calculated from MODIS *nlwv* SST and superimposed on MODIS SST image (see below for legend). Area 1 is total visible bloom area. Area 2 is the area of the red, high concentration, pixels. Dark pixels contain no data. 200 m isobath is punctured, white line.



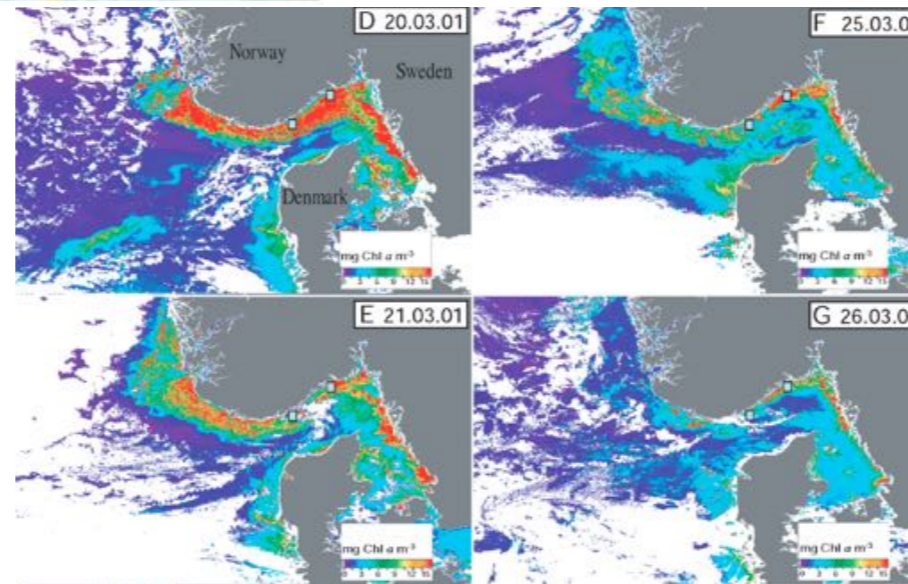
Combined remote & in situ monitoring

Country-satellite



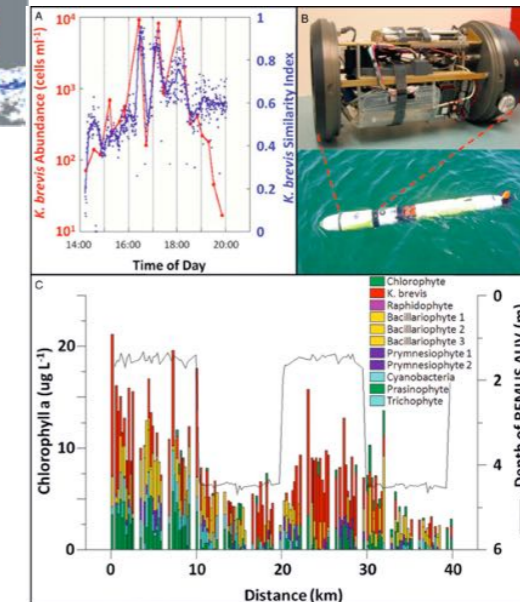
Region-satellite

Overview of phytoplankton biomass and dynamics



Local/verification - Ferrybox, AUVs

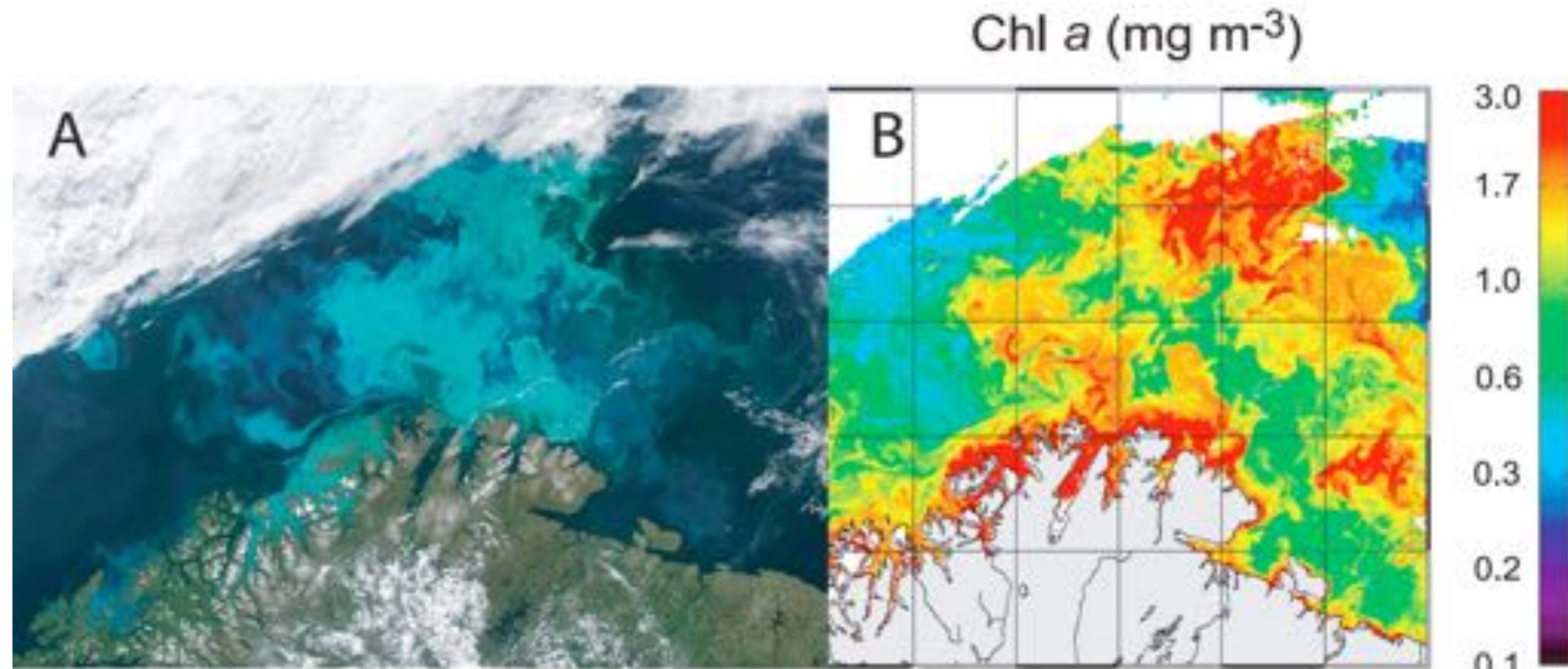
TS of Pseudo-chattonella HAB biomass and dynamics - need verification



Karenia brevis bloom in W-Florida

Bloom of *Emiliana huxleyi* in Barents Sea

Climate and watermass indicator



Johnsen et al. (2009). Ecosystem Barents Sea

Questions:

Fraction of Chl *a* from *E. huxleyi* of total
Signal from coccoliths vs cells
Other pigment groups of phytoplankton
Only signal from 1-2 m depth

Needs:

Verification of phytoplankton species and biomass
In situ verification from vessels, buoys or underwater robots

For future remote and in situ sensing of phytoplankton groups and biomass (Chl a)

Three discrete groups can be optically discriminated by ocean colour satellites (Nair et al., 2008):

1. Phycobiliprotein (Cyanobacteria)
2. Divinyl Chl a+b (Prochlorophytes)
3. Chl c-containing phytoplankton (Chromophytes), respectively

IMPORTANT: Correction algorithms in air and water:

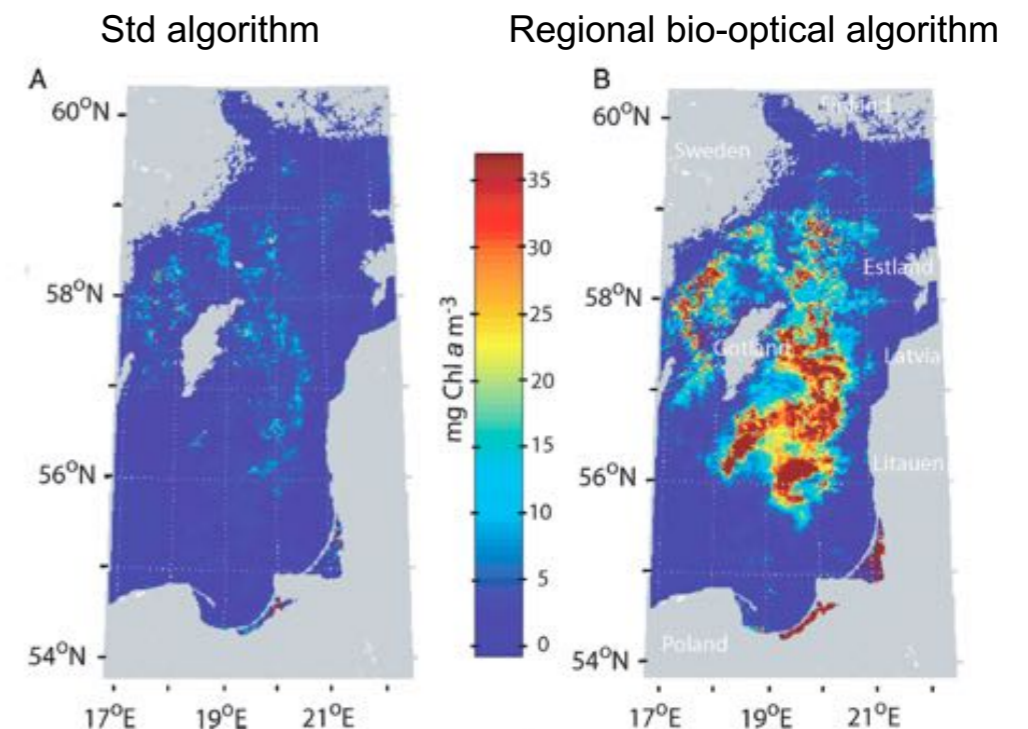
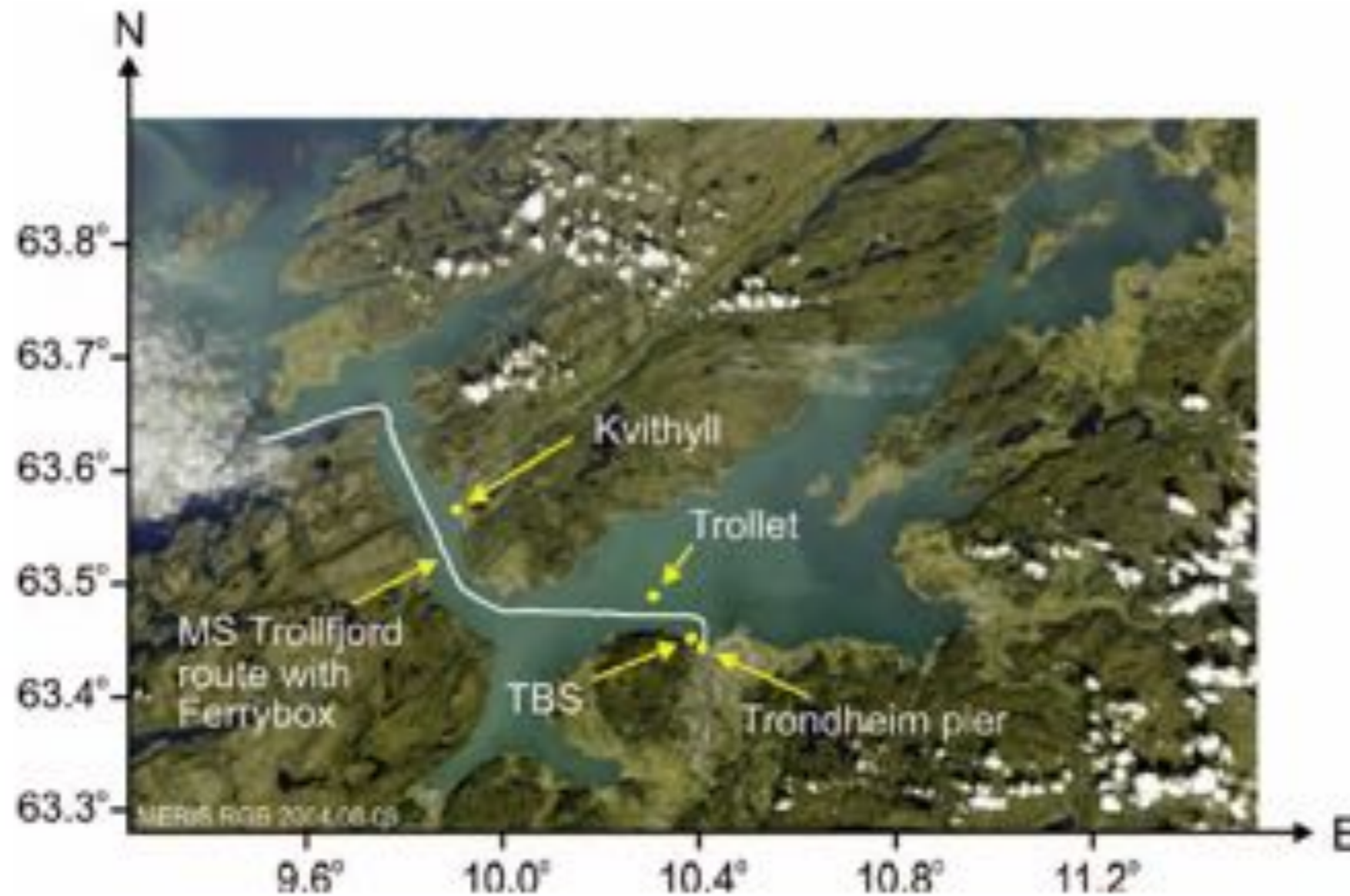


Figure 14.3. Phytoplankton biomass, seen as $C_{chl\ a}$ (mg Chl a m^{-3}), distributions across the central Baltic Sea as obtained from (A) MODIS standard product, (B) MODIS data processed with a regionally tuned bio-optical algorithm. The island in the centre of the image is Gotland. Images provided by Nansen Environmental and Remote Center (NERC).

With better **sensors, software, knowledge of pigments & bio-optical properties**, the **combined information from remote and *in situ* approaches** will probably make possible the discrimination of between 12 to 16 different bio-optical groups ---- **better biomass and taxa information**.

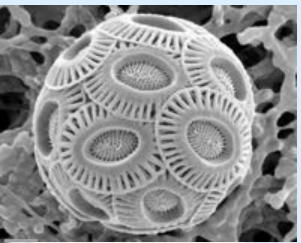
In situ & HPLC verification of satellite data



HPLC and algal sample stations: Trollet, TBS, Kvithyll and Trollet, respectively. The route of the MS Trollfjord with the Ferrybox installed onboard.

Bloom in Aug 2004

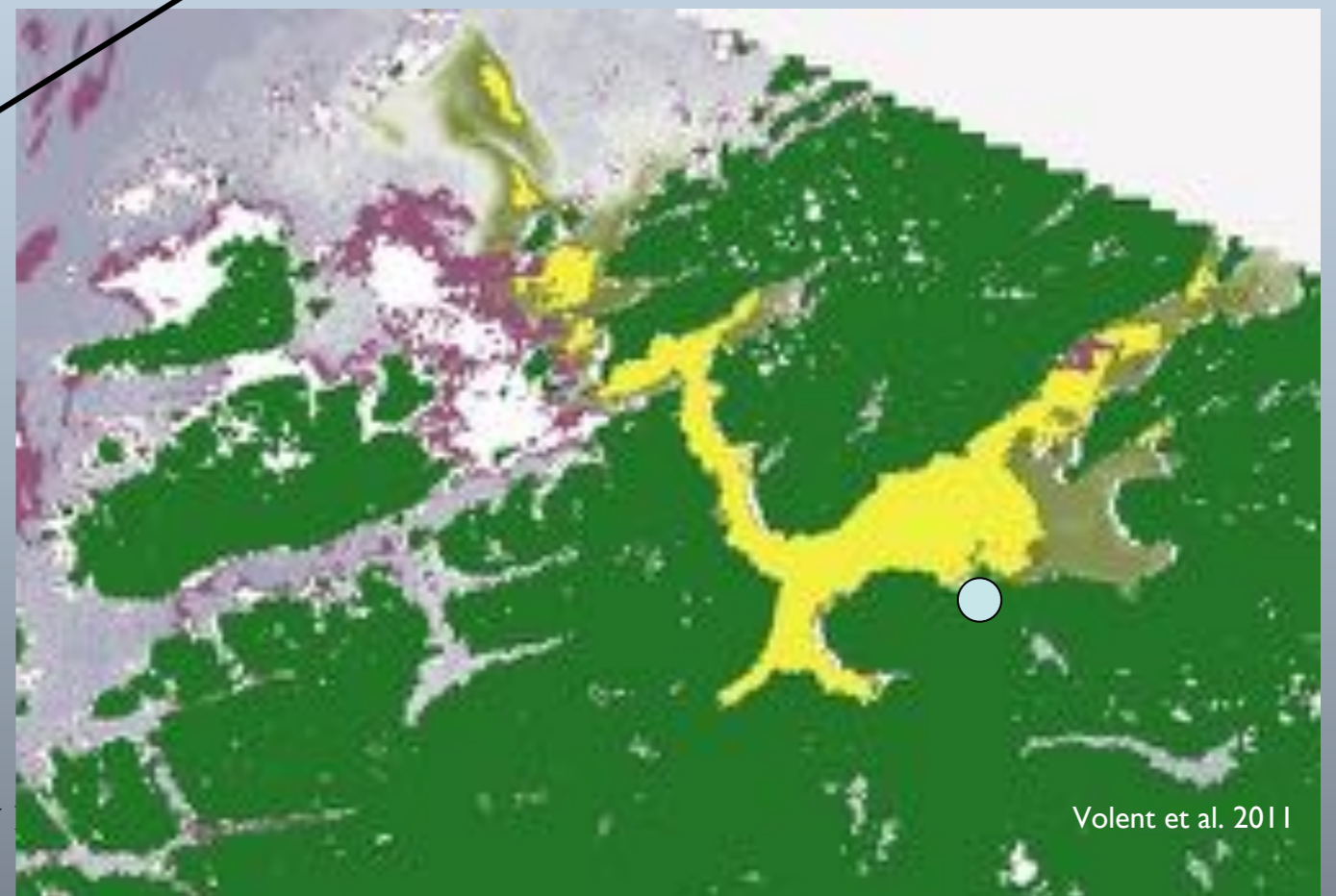
Was interpreted as «clean» *E. huxleyi*-bloom.



After 2000 - high resolution satellite images (300 m pr pixel)



radly



Volent et al. 2011

Different pigment groups of phytoplankton

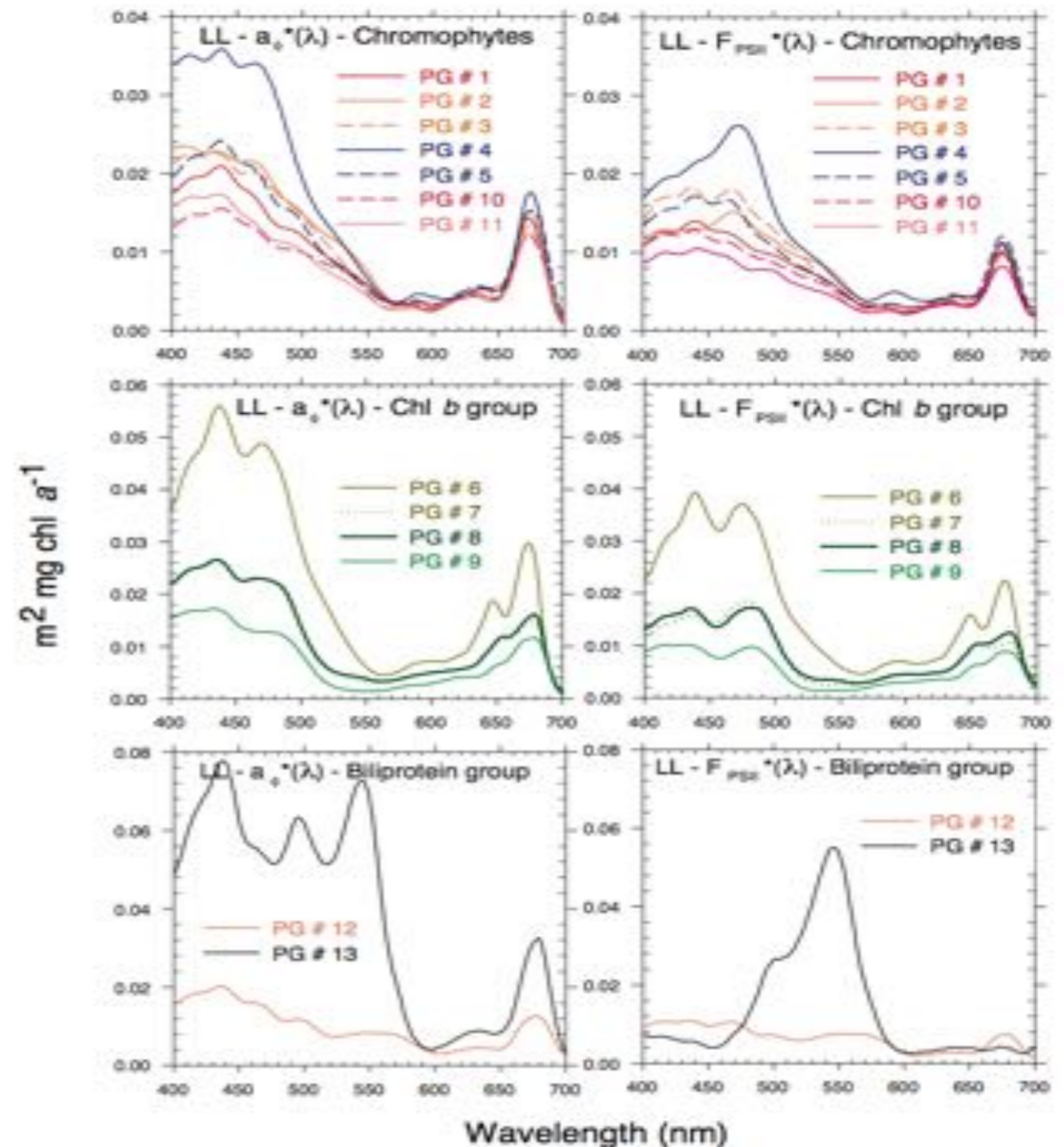
In vivo bio-optical properties in 13 PG

Bio-optical taxonomy

Pigment (chemo) taxonomy

abs

fluor

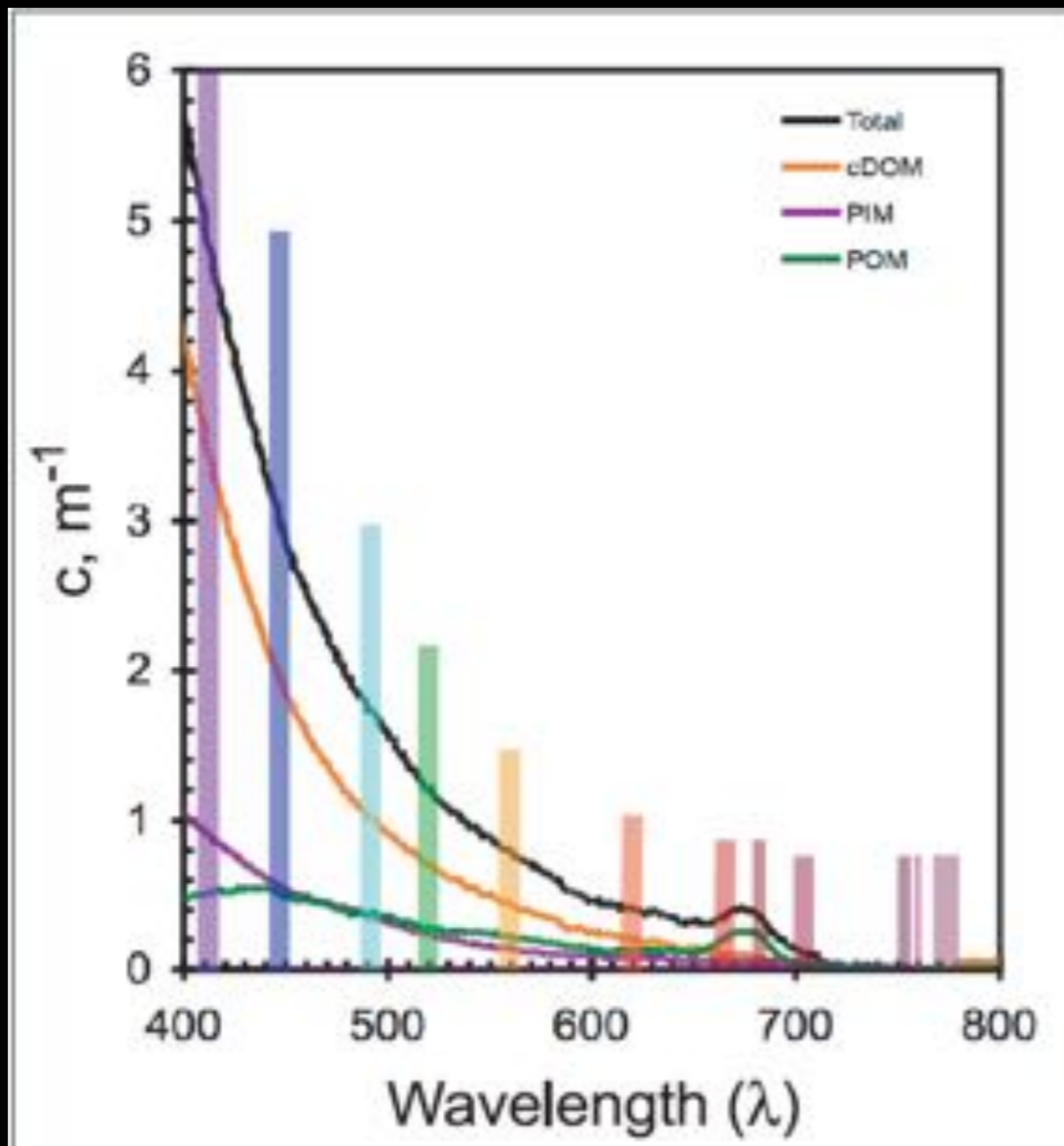


- PG 1, Bacillariophyceae (fucoxanthin, chl $c_{1,2}$): 6 species
- PG 2, Dinophyceae I (peridinin, chl c_2): 4 species
- PG 3, Dinophyceae II (acyl-oxy-fucoxanthins, gyroxanthin diester, chl c_1): 2 species
- PG 4, Coccolithophyceae (acyl-oxy-fucoxanthins, chl c_1): 8 species
- PG 5, Pavlovophyceae (fucoxanthin, chl $c_{1,2}$): 2 species
- PG 6, Prasinophyceae I (prasinoxanthin, [3,8]-proto-chlorophyllide, chl b): 3 species
- PG 7, Prasinophyceae II (lutein, chl b)
- PG 8, Euglenophyceae (neoxanthin, chl b)
- PG 9, Chlorophyceae (lutein, chl b)
- PG 10, Chrysophyceae (fucoxanthin, chl $c_{1,2}$)
- PG 11, Raphidophyceae (violaxanthin, chl $c_{1,2}$): 2 species
- PG 12, Cryptophyceae (phycobiliprotein, alloxanthin, chl c_2)
- PG 13, Cyanophyceae (phycobiliproteins, zeaxanthin)

Harmful vs benign blooms

Case II waters

Optical properties



PIM is derived mainly from freshwater run-off, mostly caused by scattering. POM, contributes both to absorption and scattering.

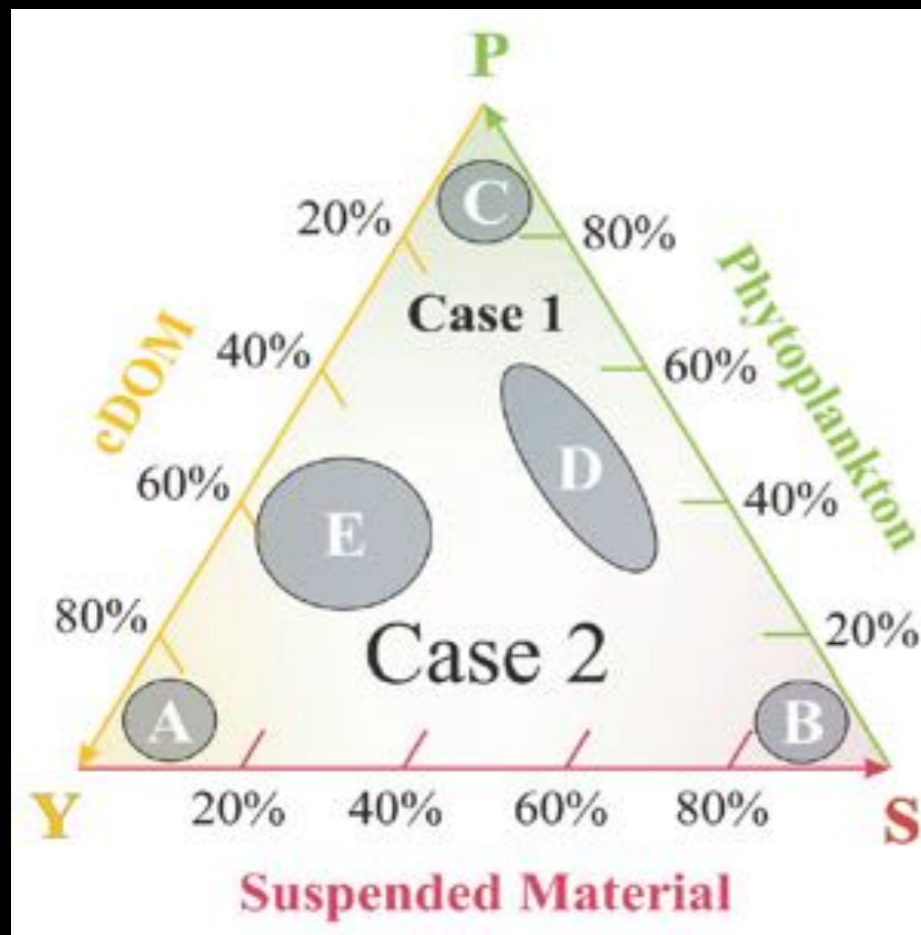
$$\text{PIM} + \text{POM} = \text{TSM}$$

Coloured bands indicate the different bandwidths of the MERIS sensor (Envisat).

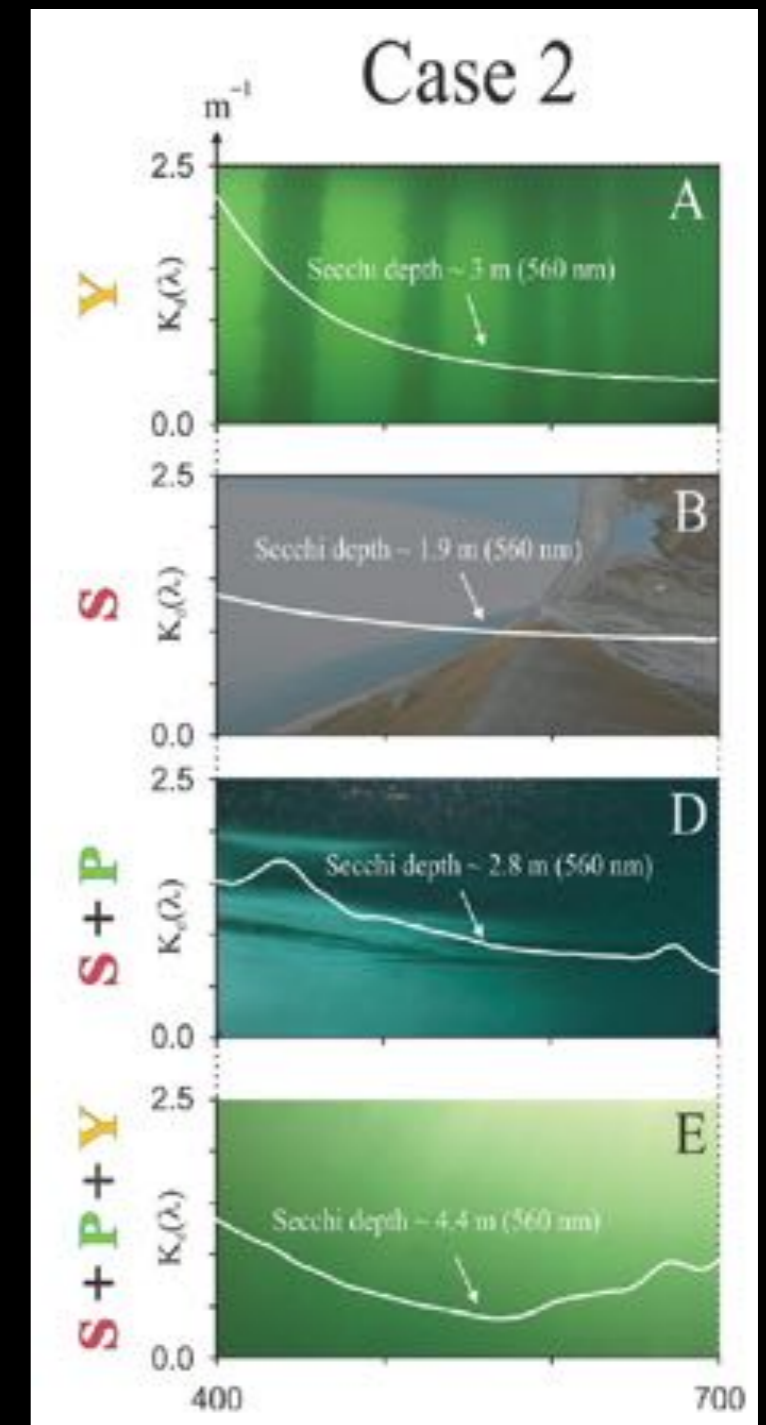
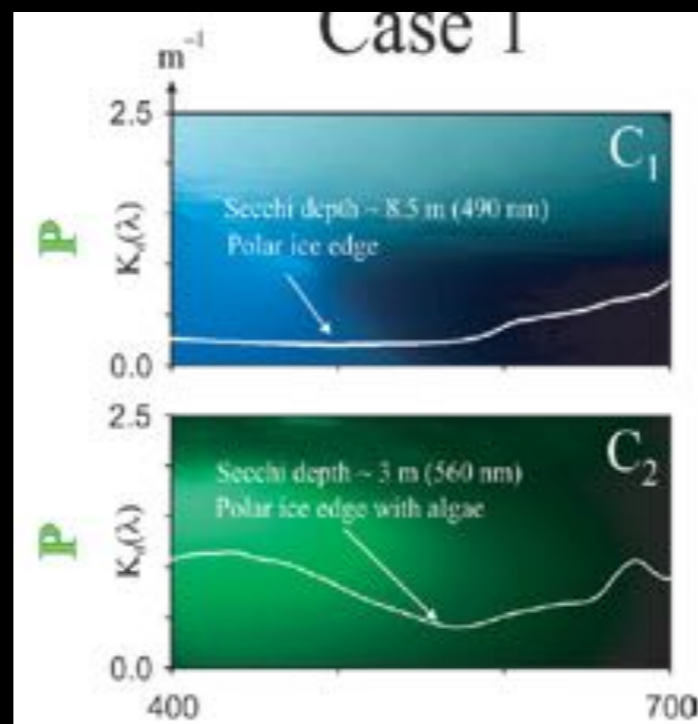
Optical properties of water depend on the spectral characteristics of:

- Water
- Phytoplankton (P)
- coloured dissolved organic matter (cDOM)
- Total suspended material (T or TSM)

Green waters
“optical complex”



Blue waters
“optical simple”





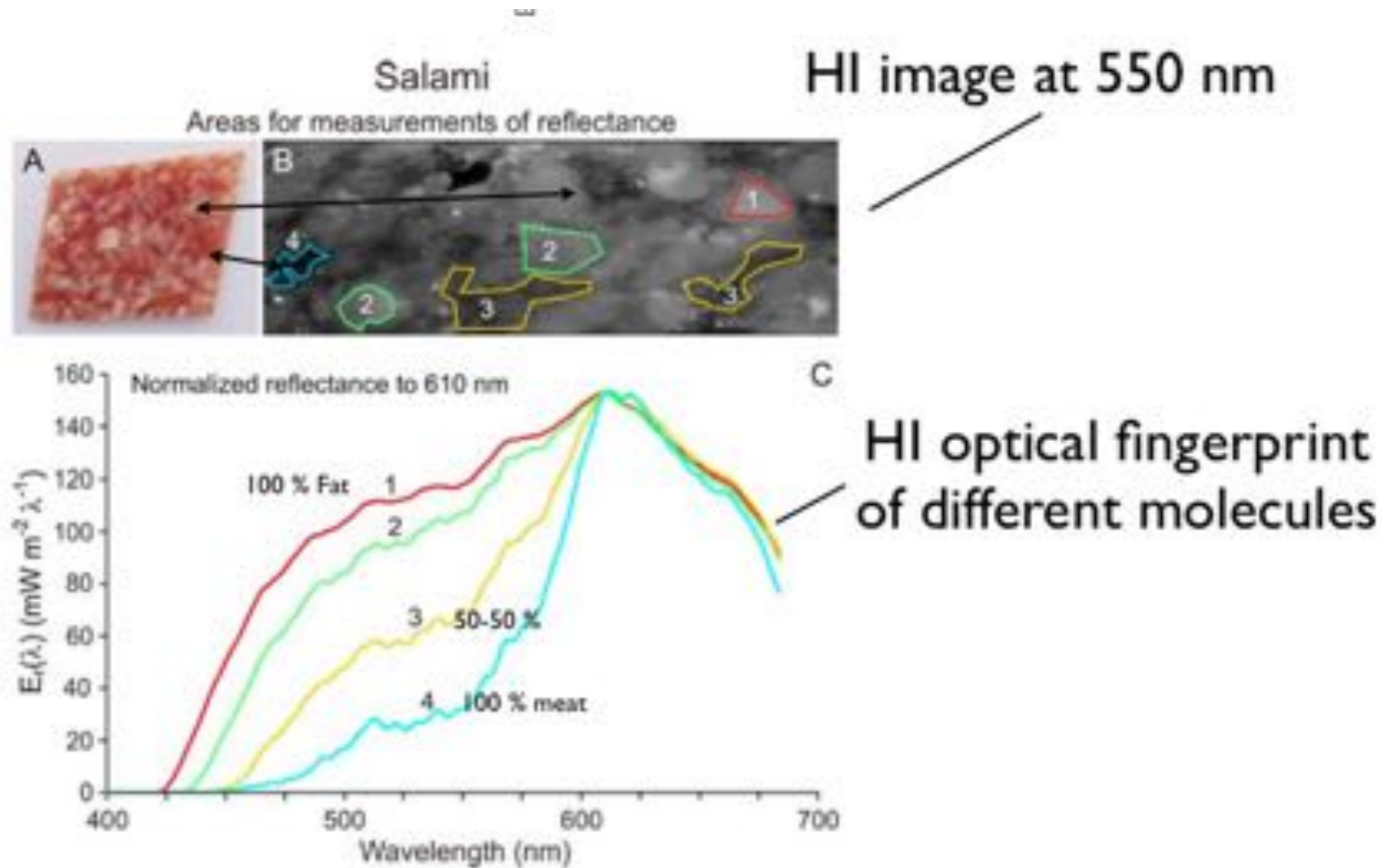
Sea, ice, clouds

Case I waters
low [Chla]

Case I waters
high [Chla]

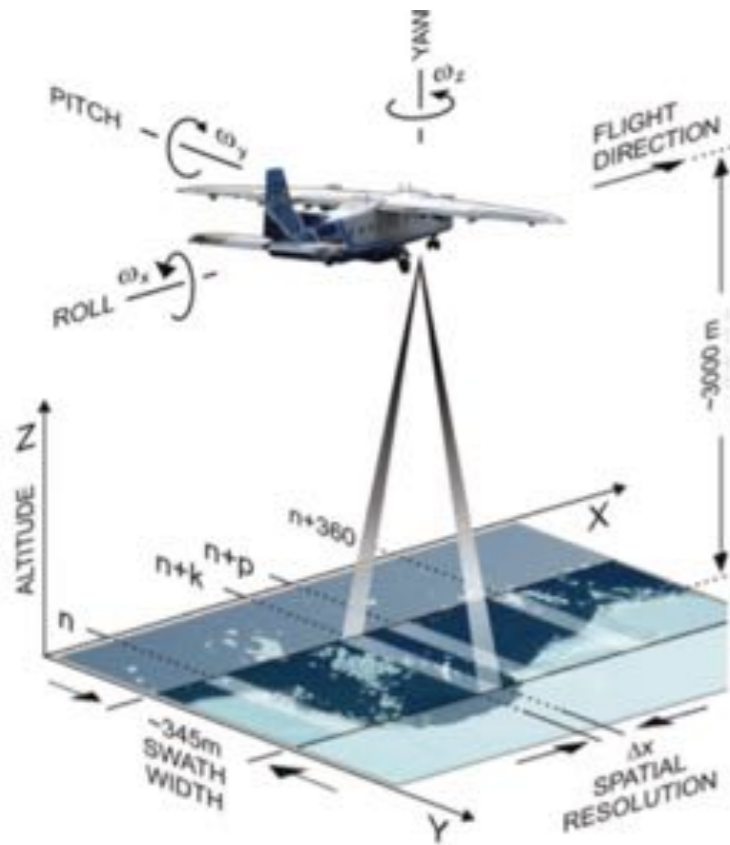
Phaeocystis bloom

Optical fingerprints of salami



Chemical imaging of fat versus muscle tissue in an Hungarian salami sausage

HI mapping of kelp forest and bottom substrate

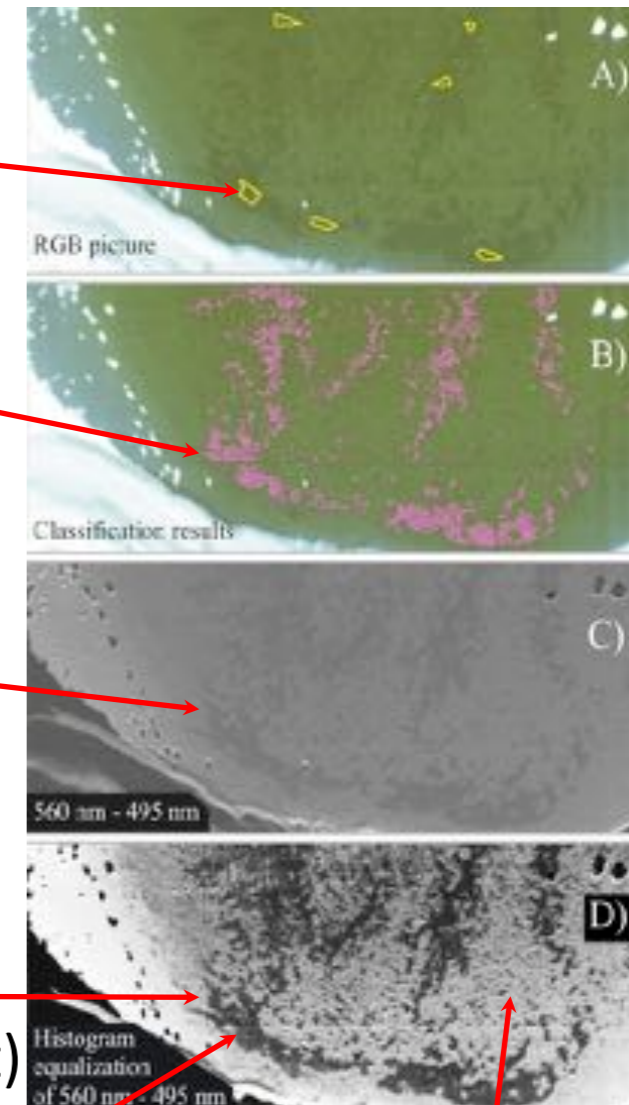


Identifying object of interest (OOI)

Classification based on optical fingerprint of OOI

$E_d(\lambda)$ penetrating deepest vs $E_d(\lambda)$ heavily absorbed by cDOM

Final classification based on optical fingerprint of kelp (*S. latissima*) and bottom substrate (fine sand & silt)

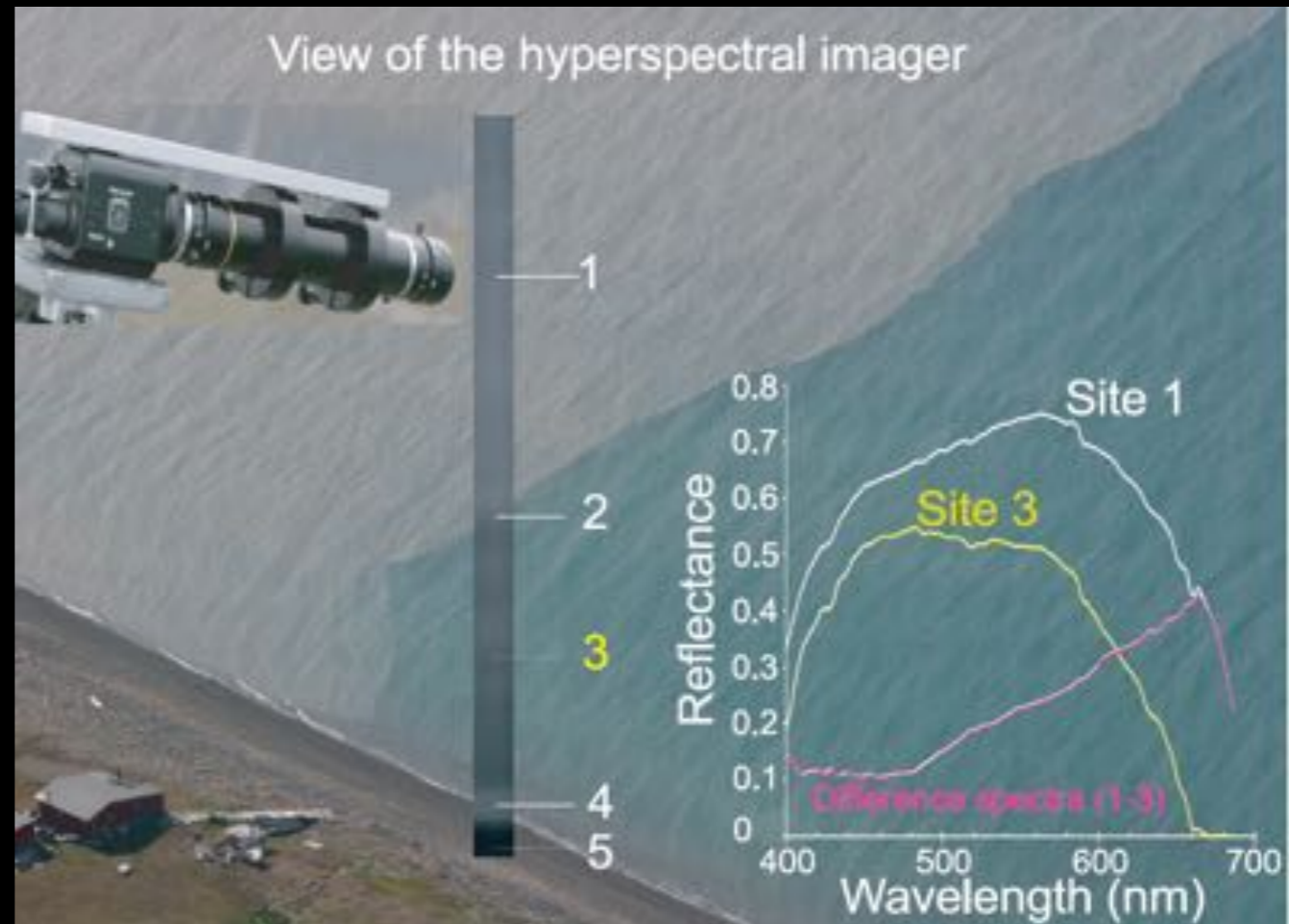
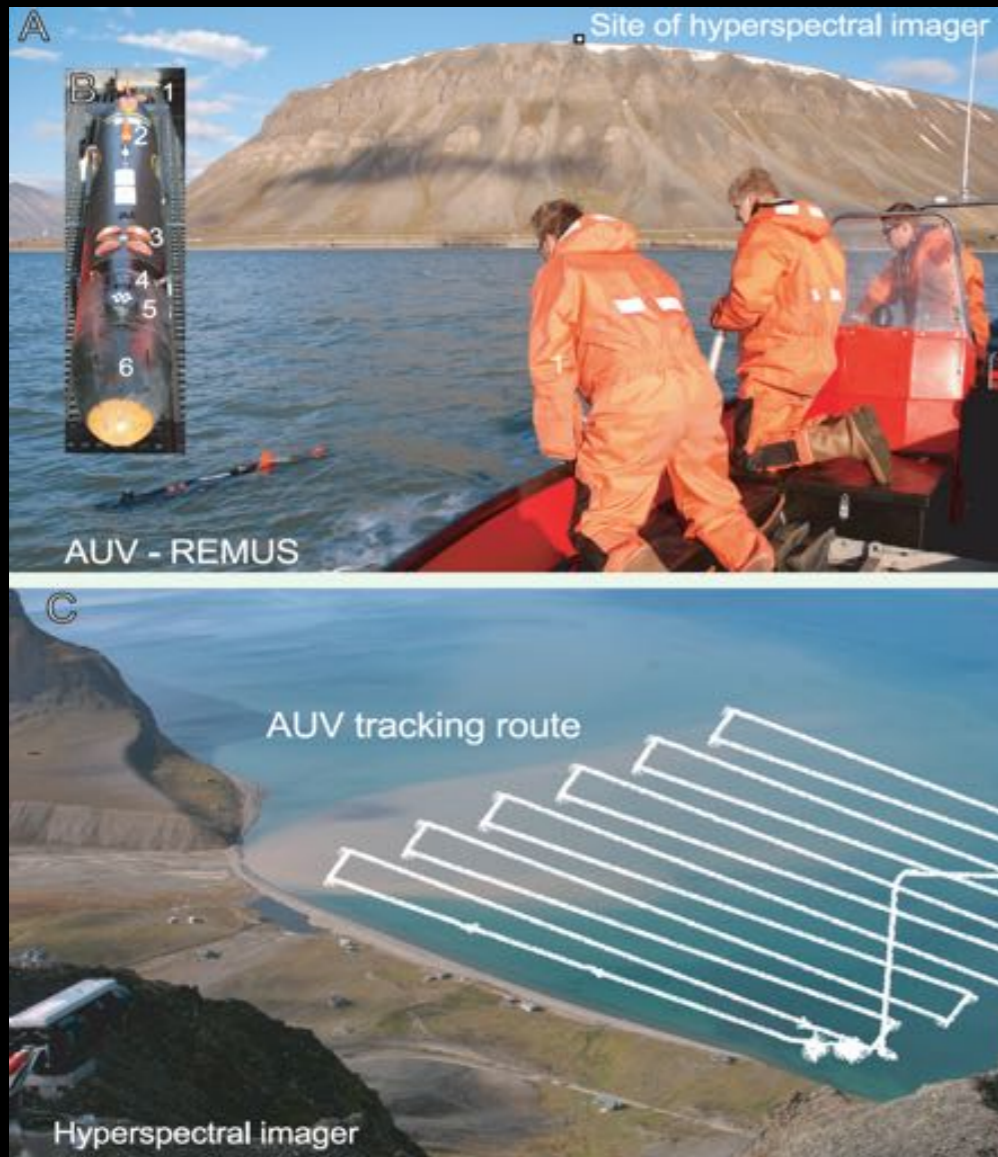


Kelp

Bottom substrate

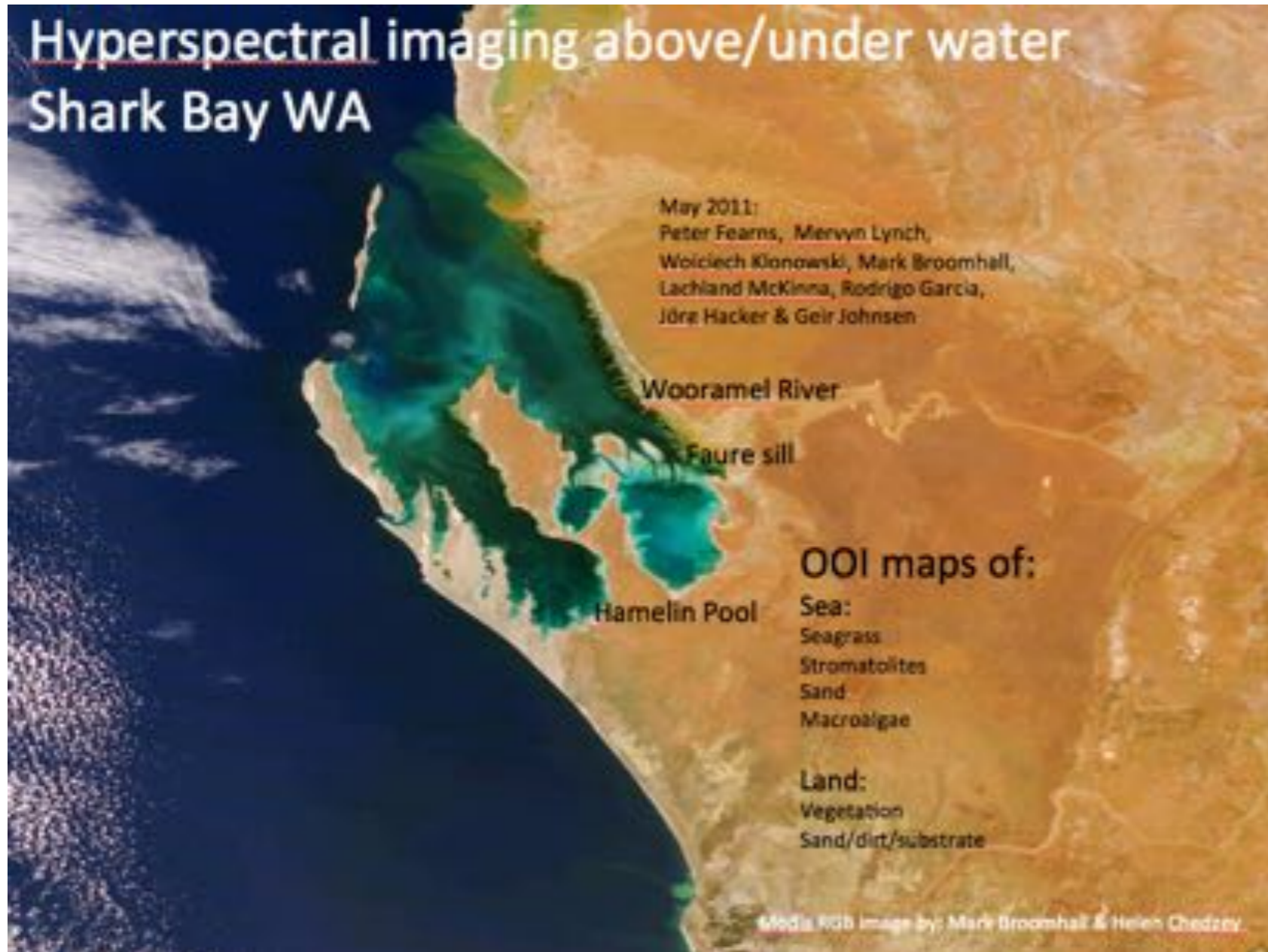
Volent, Z., Johnsen, G., & Sigernes, F. (2007). Kelp forest mapping by use of airborne hyperspectral imager. J. Appl. Remote Sensing, Vol. 1, 011503.

Remote & *in situ* sensing

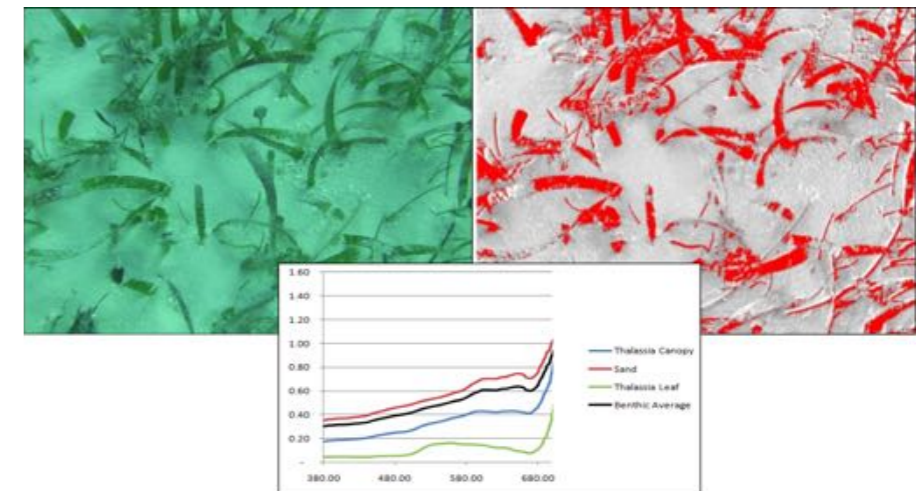


Simultaneous survey using the REMUS AUV and hyperspectral imaging of the sea surface 26 July 2007.

UHI identification, mapping & monitoring of sea grass



$$R(\lambda) = \frac{L(\lambda)_{OOI}}{L(\lambda)_{Reference}}$$

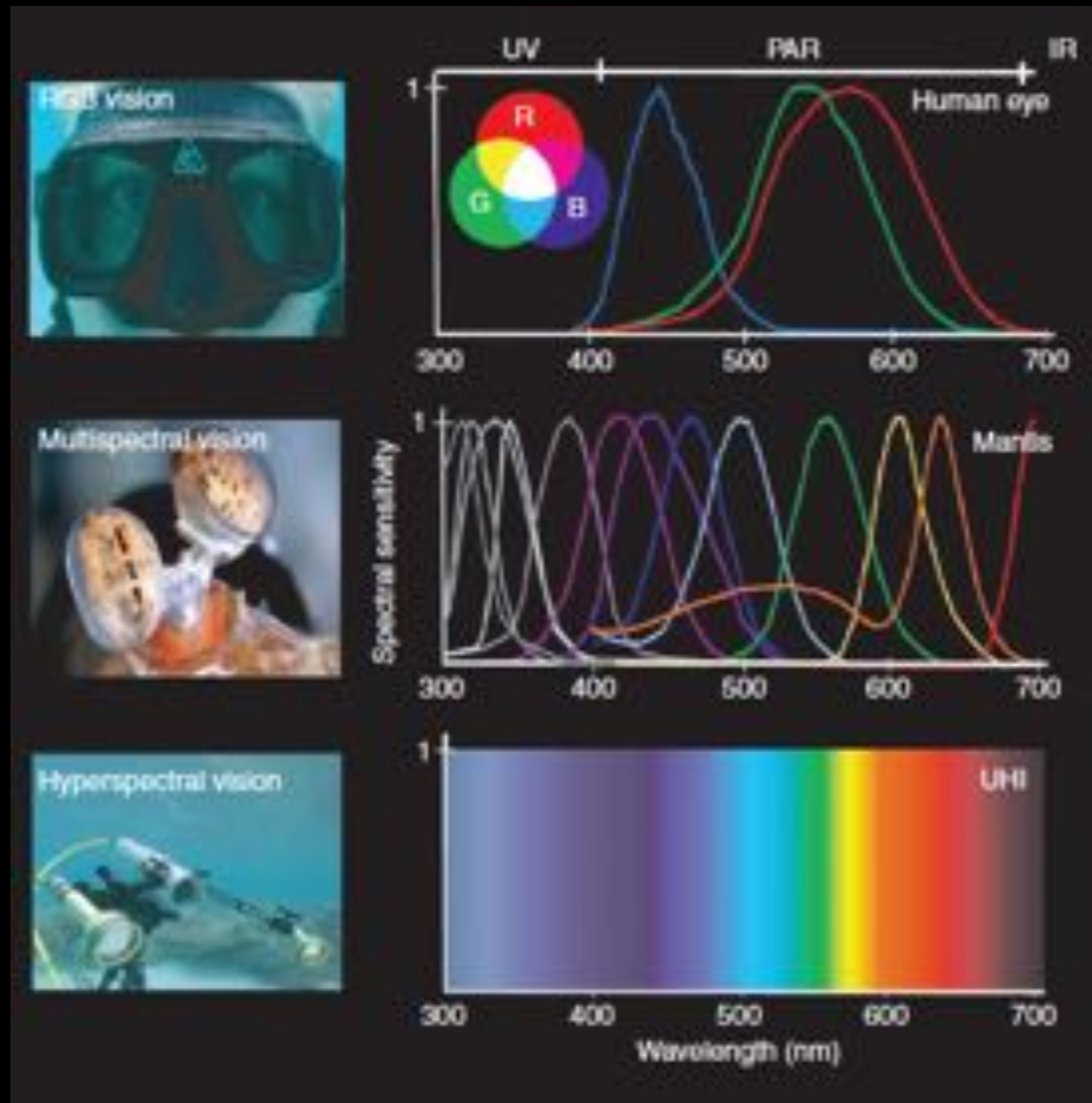


Johnsen et al. 2013

Shark Bay – covering 22000 km²

UHI-based identification and mapping of sea grass based on optical signature

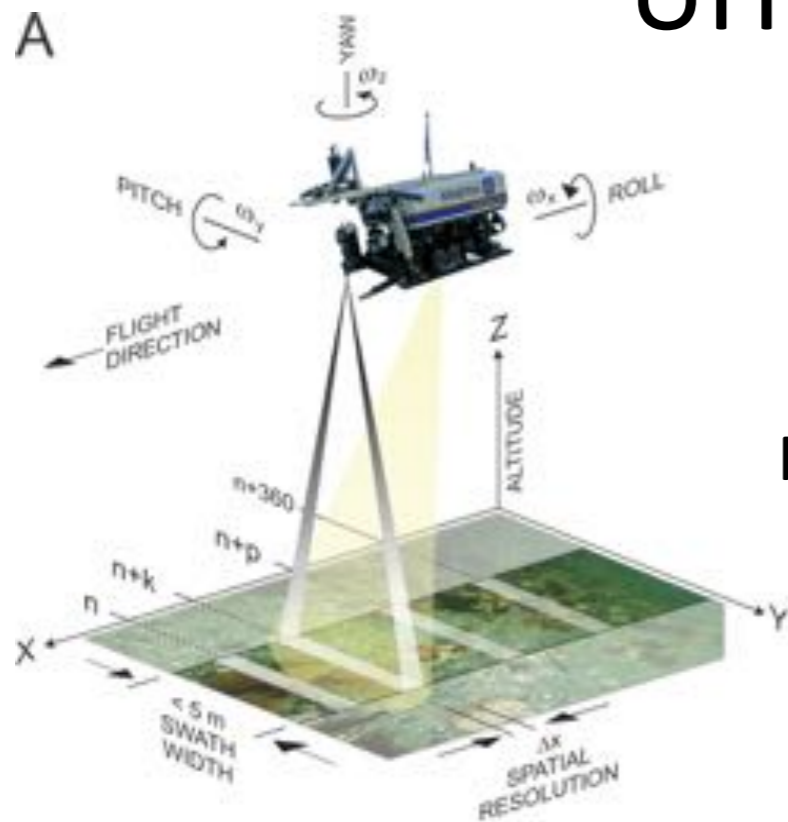
The use of underwater hyperspectral imaging (UHI) deployed on remotely operated vehicles – methods and applications



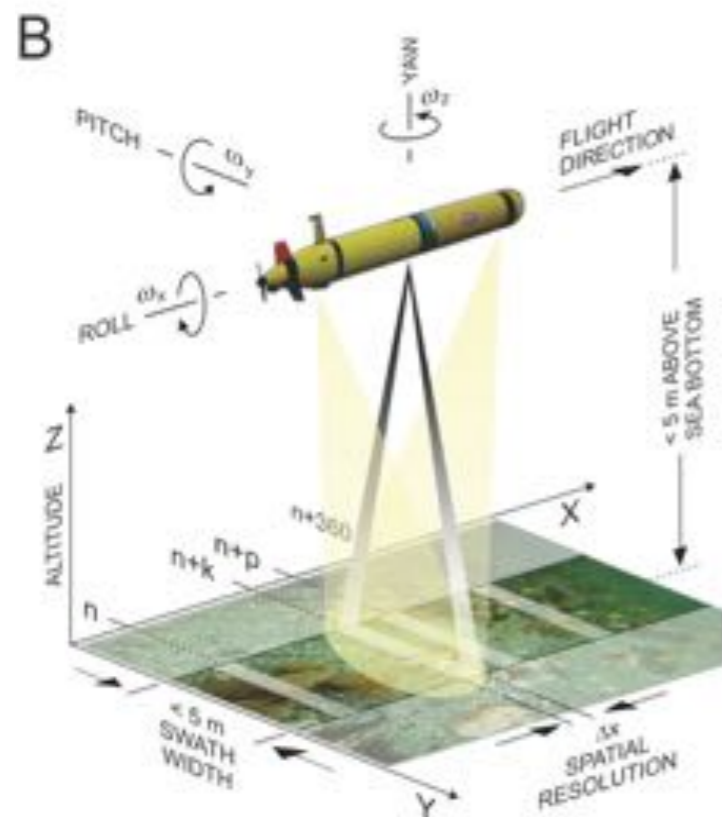
”Colour” have two components:

- Spectral resolution
- Brightness (intensity scale, bit resolution)

UHI underwater platforms



ROV – start building UHI Dec 2011 – 1 st survey April 2012

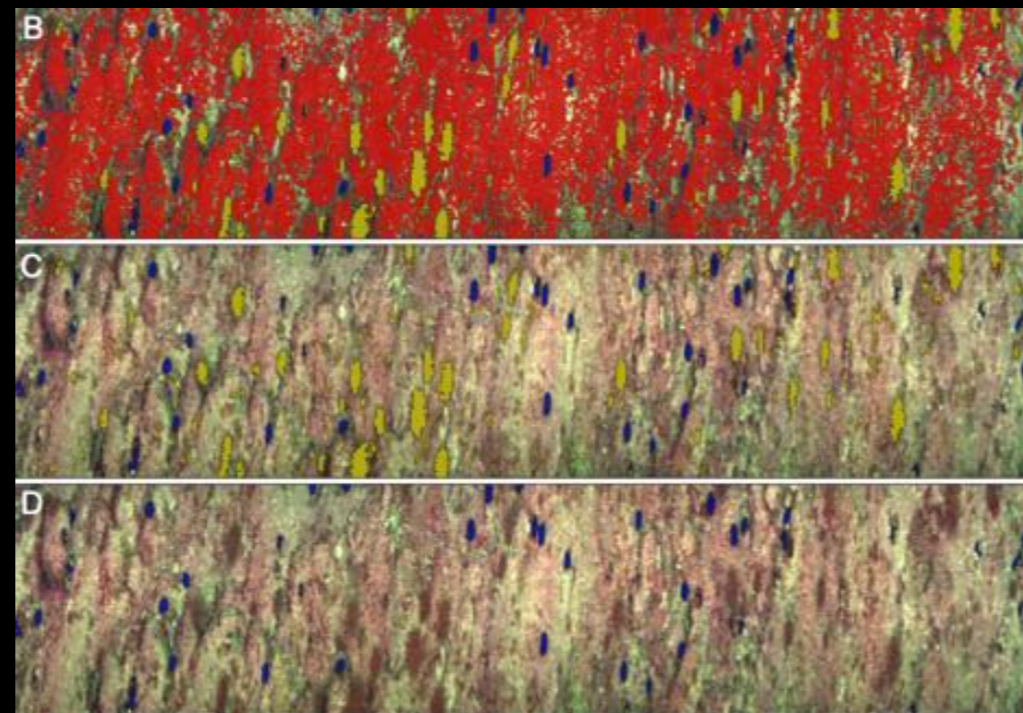
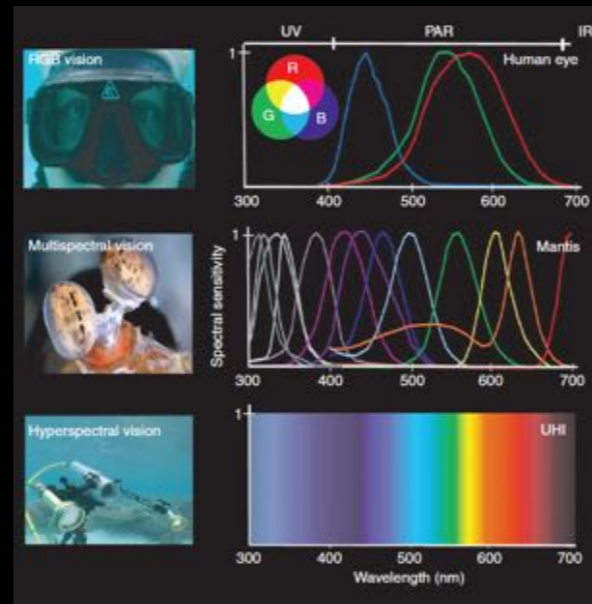
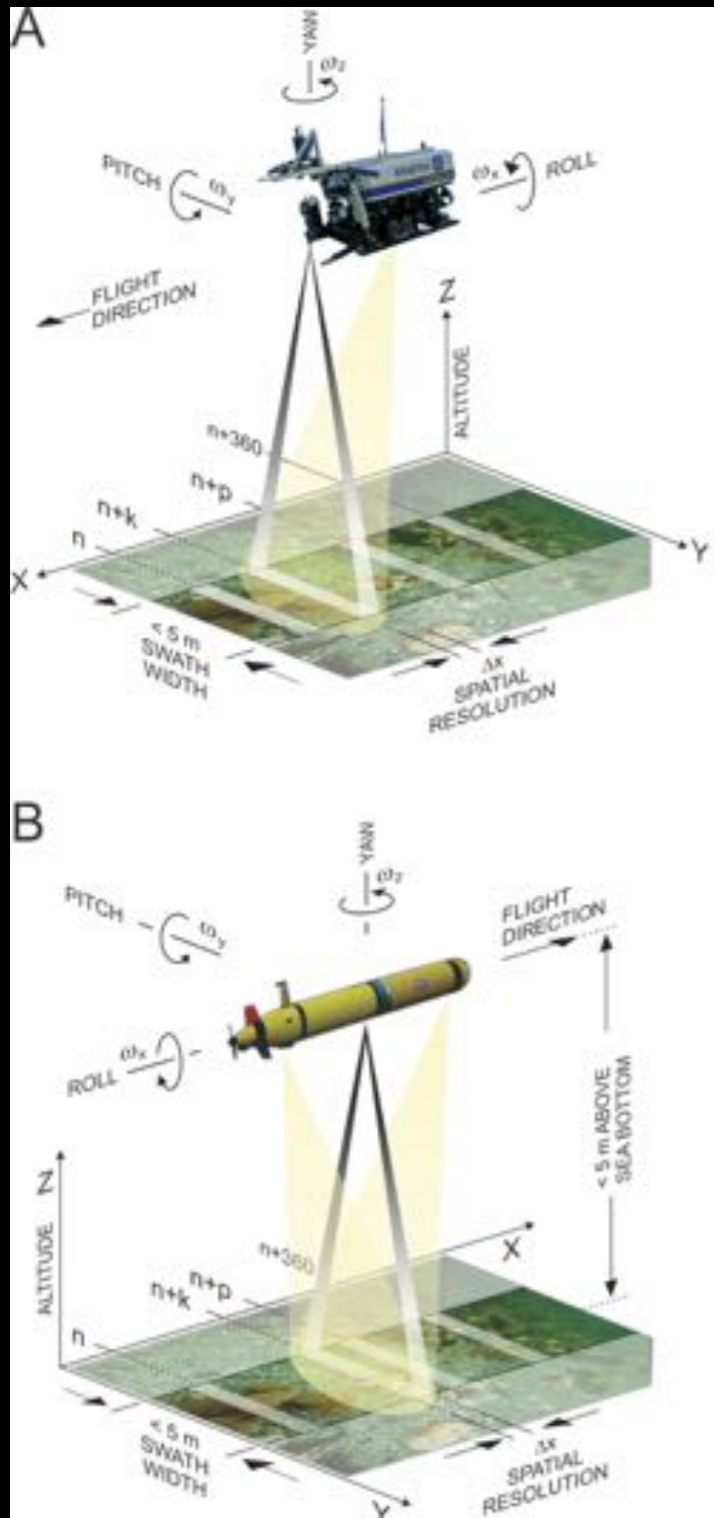


AUV – new UHI version in 2014-15 for AUV

Johansen, G., Volent, Z., Dierssen, H., Pettersen, R., Ardelan, M. V., Søreide, F., Fearn, P., Ludvigsen, M.A, Moline, M. (2013). Underwater hyperspectral imagery to create biogeochemical maps of seafloor properties. In “Subsea optics and imaging”, [Eds] Watson, J. and Zielinski, O. Woodhead Publishing Ltd., Cambridge, UK. Pp 608.

Underwater Hyperspectral Imager (UHI) på ROV og AUV

Automatisert identifikasjon, klassifisering og kartlegging av OOI

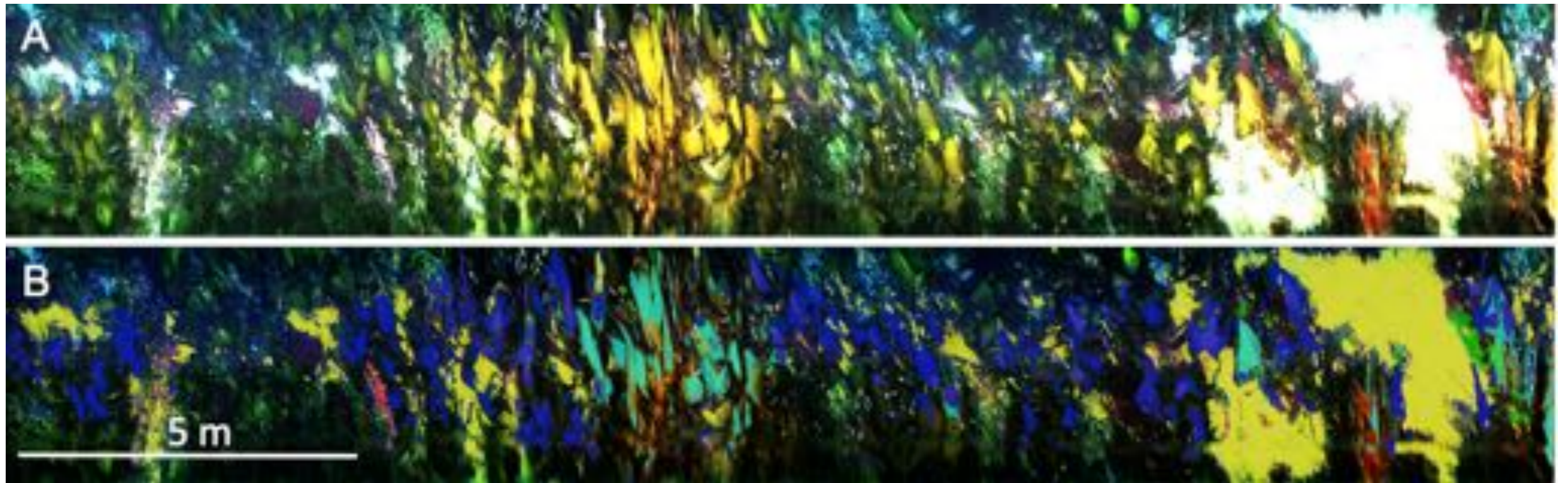


ecotone

Selskapetableringer fra fremragende forskning ved CeSOS og NTNU AMOS



UHI mapping of kelp forest – new software



UHI on ROV with false colour image (A) and (B) *supervised classification* of OOI in kelp forest. OOI-classification in B by new software and algorithms developed by Ecotone.

OOI in B are: Sand (yellow), leafy red algae (green), red calcareous algae (red), old and dark brown tissue of kelp *L. digitata* (blue) and corresponding new tissue of *L. digitata* (winter growth from meristem) are shown in magenta. Altitude was 1.5 m above kelp forest.

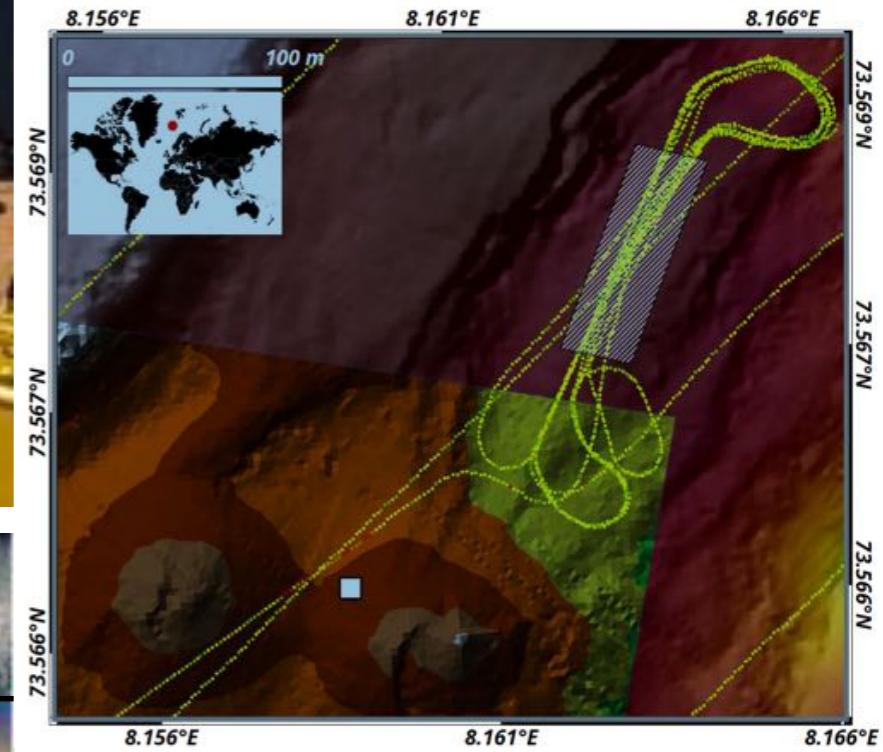
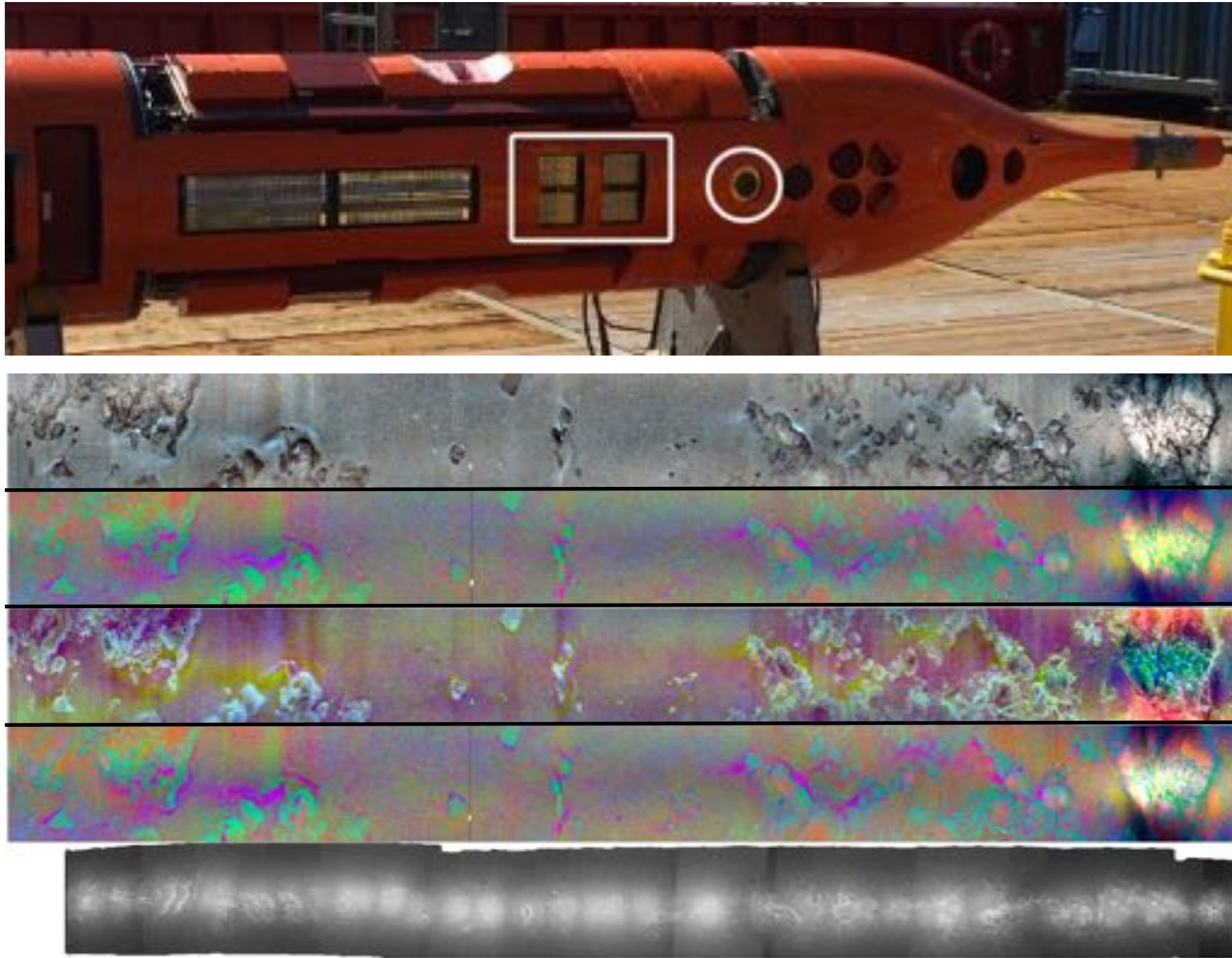


Fig. 6. UHI on AUV. From top to bottom: Pseudo-RGB, Principal component analysis (PCA), independent component analysis (ICA), factor analysis (FA) and a mosaic from another RGB camera mounted on the AUV.

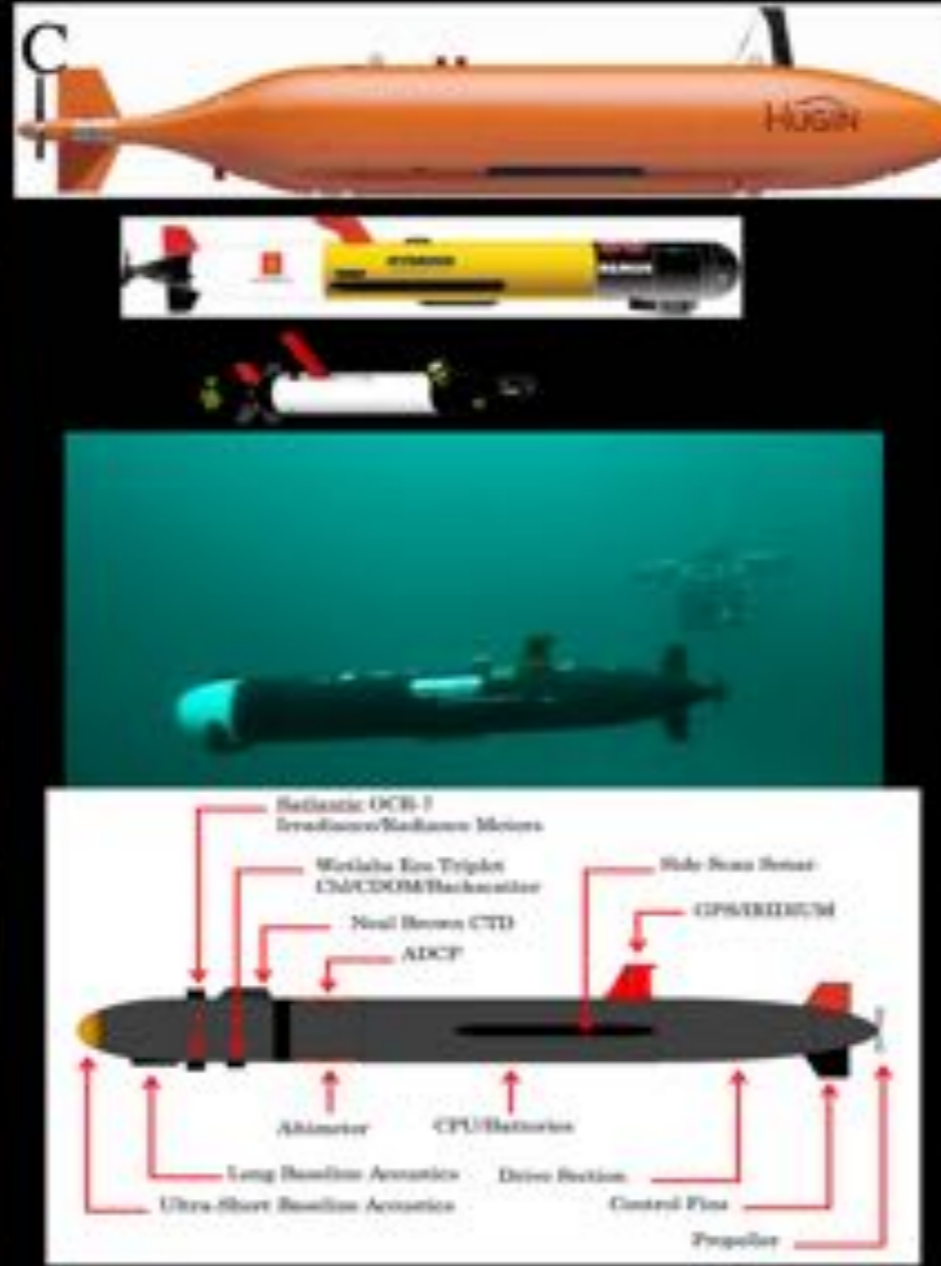
The first UHI images on AUV Hugin was acquired at the mid-Atlantic ridge in Aug 2016 with a sample rate of 10 Hz and the velocity reference of the AUV was set to 1.8ms. Sture et al. Oceans 2017.

AUTOMAP project – Marine Grunnkart i Norge - MaGIN

ROV



AUV



USV

